



Molecular Crystals and Liquid Crystals Incorporating Nonlinear Optics

Publication details, including instructions for authors and
subscription information:

<http://www.tandfonline.com/loi/gmcl17>

Reflectance Spectra of $[M(dmit)_2]$ Salts

Hiroyuki Tajima^a, Masafumi Tamura^a, Toshio Naito^a, Akiko
Kobayashi^a, Haruo Kuroda^a, Reizo Kato^b, Hayao Kobayashi^b,
Robert A. Clark^c & Allan E. Underhill^c

^a Department of Chemistry, Faculty of Science, The University of
Tokyo, Kongo, 7-3-1

^b Department of Chemistry, Faculty of Science, Toho University,
Funabashi, Chiba, 274, Japan

^c Department of Chemistry, Institute of Molecular and Biomolecular
Electronics, University of Wales, Bangor, Gwynedd, LL57 2UW, UK
Version of record first published: 22 Sep 2006.

To cite this article: Hiroyuki Tajima, Masafumi Tamura, Toshio Naito, Akiko Kobayashi, Haruo Kuroda, Reizo Kato, Hayao Kobayashi, Robert A. Clark & Allan E. Underhill (1990): Reflectance Spectra of $[M(dmit)_2]$ Salts, *Molecular Crystals and Liquid Crystals Incorporating Nonlinear Optics*, 181:1, 233-242

To link to this article: <http://dx.doi.org/10.1080/00268949008036007>

PLEASE SCROLL DOWN FOR ARTICLE

Full terms and conditions of use: <http://www.tandfonline.com/page/terms-and-conditions>

This article may be used for research, teaching, and private study purposes. Any substantial or systematic reproduction, redistribution, reselling, loan, sub-licensing, systematic supply, or distribution in any form to anyone is expressly forbidden.

The publisher does not give any warranty express or implied or make any representation that the contents will be complete or accurate or up to date. The accuracy of any instructions, formulae, and drug doses should be independently verified with primary sources. The publisher shall not be liable for any loss, actions, claims, proceedings, demand, or costs or damages whatsoever or howsoever caused arising directly or indirectly in connection with or arising out of the use of this material.

REFLECTANCE SPECTRA OF $[M(dmit)_2]$ SALTS

HIROYUKI TAJIMA, MASAFUMI TAMURA, TOSHIO NAITO, AKIKO KOBAYASHI,
and HARUO KURODA
Department of Chemistry, Faculty of Science, The University of
Tokyo, Hongo 7-3-1

REIZO KATO, and HAYAO KOBAYASHI
Department of Chemistry, Faculty of Science, Toho University,
Funabashi, Chiba, 274, Japan

ROBERT A. CLARK, and ALLAN E. UNDERHILL
Department of Chemistry and Institute of Molecular and
Biomolecular Electronics, University of Wales, Bangor, Gwynedd
LL57 2UW, UK

Abstract The polarized reflectance spectra were measured on five $[M(dmit)_2]$ salts, i.e. $Cs[Pd(dmit)_2]_2$, $Me_4As[Pd(dmit)_2]_2$, $Me_4N[Ni(dmit)_2]_2$, $Me_2Et_2N[Ni(dmit)_2]_2$, and $EDT-TTF[Ni(dmit)_2]$. Plasma frequencies, and band parameters were estimated from the spectra by use of the Drude-Lorentz model. In the two palladium salts experimental evidences were presented for the anomalous "LUMO-HOMO energy level inversion" due to strong dimerization.

INTRODUCTION

$[M(dmit)_2]$ salts ($M=Ni, Pd, Pt$) are hopeful candidates for the molecular superconductor together with TTF derivatives' salts. Until now four $[M(dmit)_2]$ salts are known to become superconductors under pressure.¹⁻³ The calculation of molecular orbital showed that the LUMO of $[M(dmit)_2]$, expected to form conduction band, has b_{2g} symmetry² while the HOMO with b_{1u} symmetry forms the conduction band in the cases of the TTF derivatives' salts.² This implies that the character of S-S interaction in this system is expected to be different from that in BEDT-TTF or other TTF derivatives. Moreover anomalous LUMO-HOMO energy level inversion was recently suggested from the band structure calculation of $Cs[Pd(dmit)_2]_2$. However, few experimental evidences for the predicted band structures have been hitherto reported. In this article we show the results of optical study on five $[M(dmit)_2]$ salts to examine the band structures.

Results

$\text{Me}_4\text{N}[\text{Ni}(\text{dmit})_2]_2$

In this salt, there are two types of conduction sheets. One has the stacking axis parallel to the $[110]$ (see Fig. 1(a)), the other parallel to the $[\bar{1}10]$ axis. Each conduction sheet is separated by the cation, Me_4N^+ , with the repeating distance, $c/2$. Figure 1(b) shows the reflectance spectra for the light polarization parallel to the a -axis and b -axis which are the principal axes of the monoclinic lattice. It was reported that the resistivity of this salt raises in low temperature region under ambient pressure and the temperature dependence of the resistivity varies from sample to sample.^{2,4} But the measured reflectance spectra look Drude-like down to 20K and any

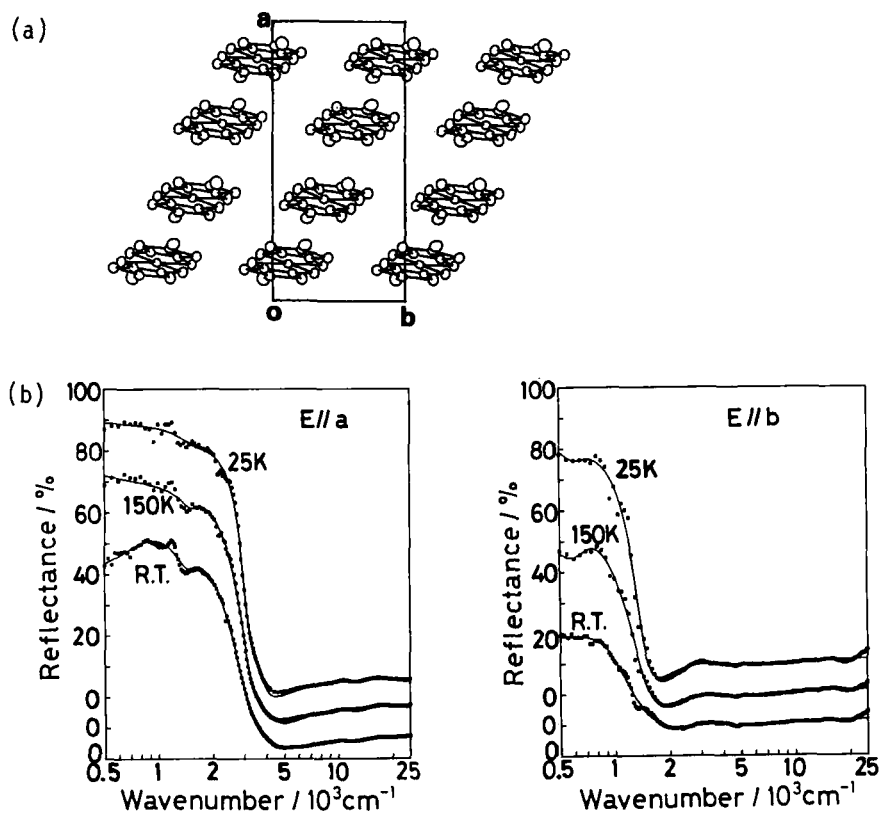


FIGURE 1 (a) Crystal structure and (b) reflectance spectra of $\text{Me}_4\text{N}[\text{Ni}(\text{dmit})_2]_2$. The solid line in Fig. 1(b) represents the Drude-Lorentz fit to the reflectance spectra.

sample dependence was not observed.⁵ This suggests the resistivity anomaly frequently observed in this material is not the inherent behavior. The plasma frequencies for the infrared metallic dispersions were obtained from the reflectance spectra by use of the Drude-Lorentz model assuming the complex dielectric function $\varepsilon(\omega)$ expressed by the following equation,

$$\varepsilon(\omega) = \varepsilon_c - \omega_p^2 / (\omega^2 + i\gamma\omega) - \sum_j \Omega_{pj}^2 / (\omega^2 - \omega_j^2 + i\Gamma_j\omega) \quad (1)$$

where ε_c , ω_p , γ and $[\omega_j, \Omega_{pj}, \Gamma_j]$ denote the back ground dielectric constant, the plasma frequency of intra-band transition, the relaxation rate of the free carriers and the parameters of the Lorentz oscillator for the j -th excitation, respectively. The obtained plasma frequencies are $5.5 \times 10^3 \text{ cm}^{-1}$ (ω_{pa}) for the //a spectrum and $3.2 \times 10^3 \text{ cm}^{-1}$ (ω_{pb}) for the //b spectrum. Due to the molecular arrangement in Fig. 1(a), both the //a and //b spectra include the component parallel and perpendicular to the stacking axis. Therefore it is necessary to deduce the plasma frequency parallel and perpendicular to the stacking axis ($\omega_{p//}$, $\omega_{p\perp}$) in order to estimate the anisotropy within ab-plane. It was made by solving the following simultaneous equation,

$$\begin{aligned} \omega_{pa}^2 &= \omega_{p//}^2 \cos^2 \theta + \omega_{p\perp}^2 \sin^2 \theta \\ \omega_{pb}^2 &= \omega_{p//}^2 \sin^2 \theta + \omega_{p\perp}^2 \cos^2 \theta \end{aligned} \quad (2)$$

where θ is the angle between the a-axis and the stacking axis. Thus obtained plasma frequencies ($\omega_{p//}$, $\omega_{p\perp}$) are $6.0 \times 10^3 \text{ cm}^{-1}$ and $2.0 \times 10^3 \text{ cm}^{-1}$, respectively. If we assume the effective transfer integrals parallel and perpendicular to the stacking axis, they are estimated to be 0.10 eV, and 0.02 eV by use of the ($\omega_{p//}$, $\omega_{p\perp}$) values. These values of transfer integrals are consistent with the results of extended Hückel calculations.⁴

Cs[Pd(dmit)₂]₂

The crystal structure of this material is similar to Me₄N[Ni(dmit)₂]₂. The degree of dimerization is much stronger than the latter, and besides there are short S-S contacts between conducting sheets mediated by the terminal thiones.⁶ Figure 2 shows the

temperature dependence of the reflectance and conductivity spectra for the light polarization parallel to the a-axis and b-axis. The reflectance spectra include three characteristic dispersions. They are Drude-like dispersion below $3 \times 10^3 \text{ cm}^{-1}$ commonly observed in the organic metals, weak dispersion about $4 \times 10^3 \text{ cm}^{-1}$ and strong dispersion around $11 \times 10^3 \text{ cm}^{-1}$, respectively. The first dispersion is fairly isotropic within the ab-plane in comparison with $\text{Me}_4\text{N}[\text{Ni}(\text{dmit})_2]_2$ salt. Its line shape changes below 50K to the one that indicates the gap formation due to metal-insulator transition ($T_{\text{MI}}=60\text{K}$).⁶ The second dispersion is observed only in the //a spectrum. Similar dispersion was also observed in the spectrum of $\text{Me}_4\text{N}[\text{Ni}(\text{dmit})_2]_2$, and $\text{Me}_4\text{As}[\text{Pd}(\text{dmit})_2]_2$. The third dispersion is strongly polarized along

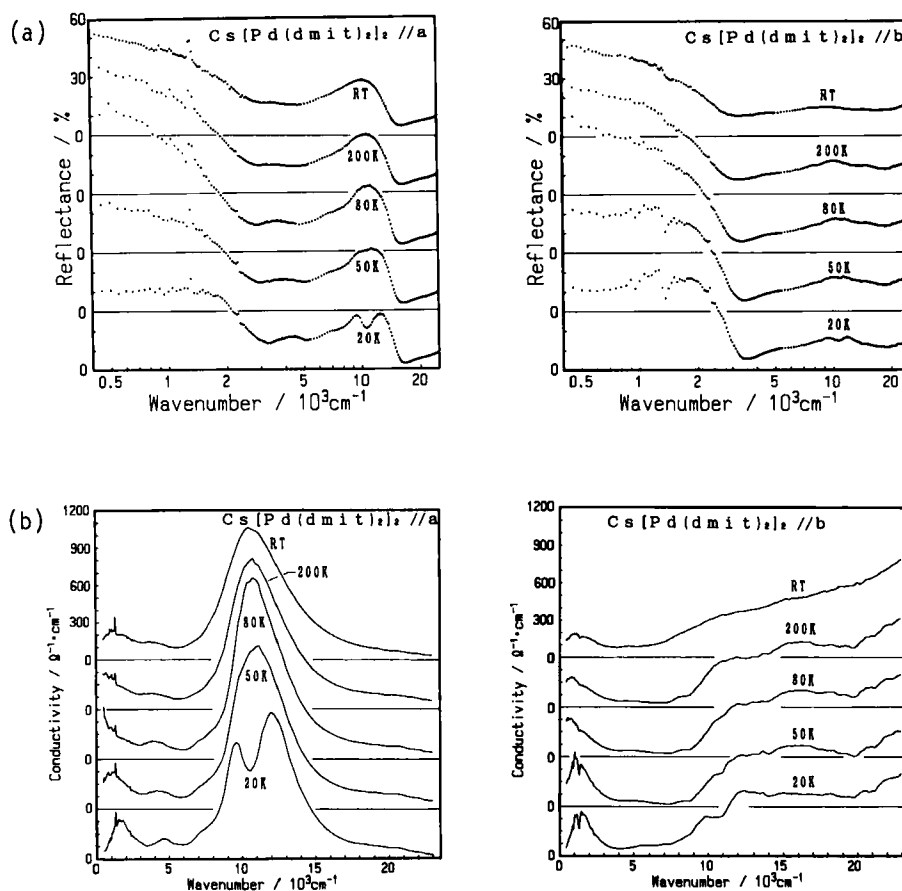


FIGURE 2 (a) Reflectance spectra and (b) conductivity spectra of $\text{Cs}[\text{Pd}(\text{dmit})_2]_2$.

the a-axis, which splits into two bands below the phase transition temperature. We analyzed the reflectance spectrum by use of the Drude-Lorentz model (Eq. (1)). In the curve fitting procedure we neglect the dispersion around $4 \times 10^3 \text{ cm}^{-1}$, since this has small intensity, and its line shape was hardly reproduced by the Lorentz function. The obtained plasma frequencies for the intra-band transition are $6.0 \times 10^3 \text{ cm}^{-1} (//a)$ and $6.2 \times 10^3 \text{ cm}^{-1} (//b)$, respectively at 80K. These values show isotropic nature of the electronic structure in this material in contrast with $\text{Me}_4\text{N}[\text{Ni}(\text{dmit})_2]_2$.

$\text{Me}_4\text{As}[\text{Pd}(\text{dmit})_2]_2$

This salt is isostructural with $\text{Cs}[\text{Pd}(\text{dmit})_2]_2$.⁷ The crystal

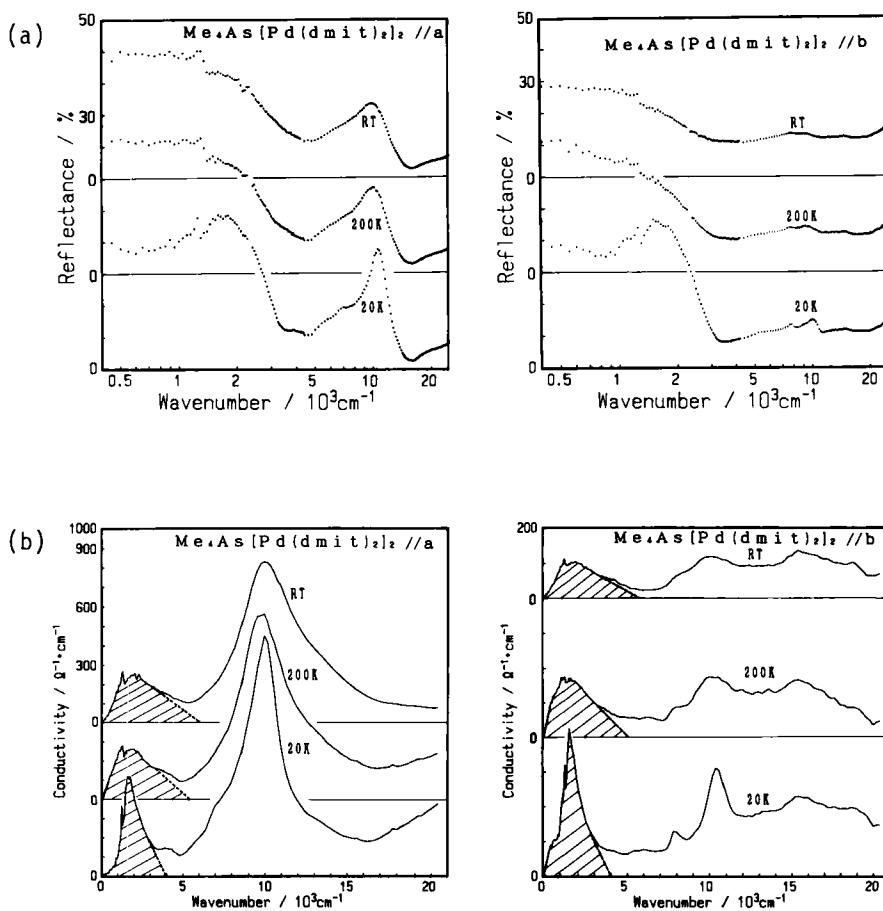


FIGURE 3 (a) Reflectance spectra and (b) conductivity spectra of $\text{Me}_4\text{As}[\text{Pd}(\text{dmit})_2]_2$.

structure within the conduction sheet is almost same as that of the Cs salt, but the interaction between terminal thiones is negligible in this salt due to the bulky Me_4As^+ . Contrary to the Cs salt, the electronic property of this material is semiconductive even at room temperature. This is against the prediction from the simple tight binding calculation. Electron-electron interaction seems to play an important role in this material. Figure 1 shows the reflectance and conductivity spectra of this material. The broad dispersion about $10 \times 10^3 \text{cm}^{-1}$ appears in this salt as well as in $\text{Cs}[\text{Pd}(\text{dmit})_2]_2$ salt. The conductivity spectra show the existence of an energy gap even at room temperature, and the gap becomes clearer on lowering the temperature. The plasma frequencies in the infrared region are calculated by integrating shaded area of the conductivity spectra. The results are [$5.6 \times 10^3 \text{cm}^{-1}$ (R.T.), $5.6 \times 10^3 \text{cm}^{-1}$ (200K), $5.4 \times 10^3 \text{cm}^{-1}$ (20K)] for the //a spectra, and [$3.5 \times 10^3 \text{cm}^{-1}$ (R.T.), $4.3 \times 10^3 \text{cm}^{-1}$ (200K), $4.9 \times 10^3 \text{cm}^{-1}$ (20K)] for the //b spectra, respectively. It should be noted that the significant increase of the plasma frequency was observed for the //b spectrum with a decrease in temperature.

$\text{Et}_2\text{Me}_2\text{N}[\text{Ni}(\text{dmit})_2]$

This material is metallic down to 1.5K, but does not exhibit superconductivity.⁸ Reflectance spectra were measured within the bc-plane for the polarization parallel to the a-axis and c-axis. Figures 4(a) and 4(b) show the crystal structure within the bc-plane and the reflectance spectra, respectively. Drude-like dispersions appear for both polarizations. A dispersion about $4 \times 10^3 \text{cm}^{-1}$ grows up with a decrease in temperature. The plasma frequencies at 25K were estimated to be $4.2 \times 10^3 \text{cm}^{-1}$ (//b), and $5.9 \times 10^3 \text{cm}^{-1}$ (//c), respectively, by use of Eq. (1). The optical masses were calculated to be $5.9m_e$ (//b) and $3.0m_e$ (//c), respectively, by use of these plasma frequencies.

The calculation of the transfer integrals based on the extended Huckel method suggested that the two transfer integrals, which are depicted p_1 , p_3 in Fig. 4a, excel others. Hence we adopt the simplified band structure, neglecting all the transfer integral except for p_1 and p_3 . By virtue of this simplification the energy dispersion is described by the following equation,

$$\varepsilon(k) = \pm (p_3^2 + 2p_1^2(1 + \cos k \cdot b) \pm 4p_3p_1 \cos(k \cdot b/2) \cos(k \cdot c/2))^{1/2} \quad (3)$$

The plasma frequencies are calculated by

$$\omega_{px}^2 = (e^2 / \pi^2 \hbar^2) \int \partial^2 \varepsilon / \partial k_x^2 f(k) dk \quad (4)$$

where subscript x represents the direction of either a -axis or b -axis, and $f(\varepsilon)$ is the Fermi distribution function. By use of these equations transfer integrals were estimated from the plasma frequencies to be 0.10 eV (p_1), and 0.12 eV (p_3). Figure 4(c) shows the

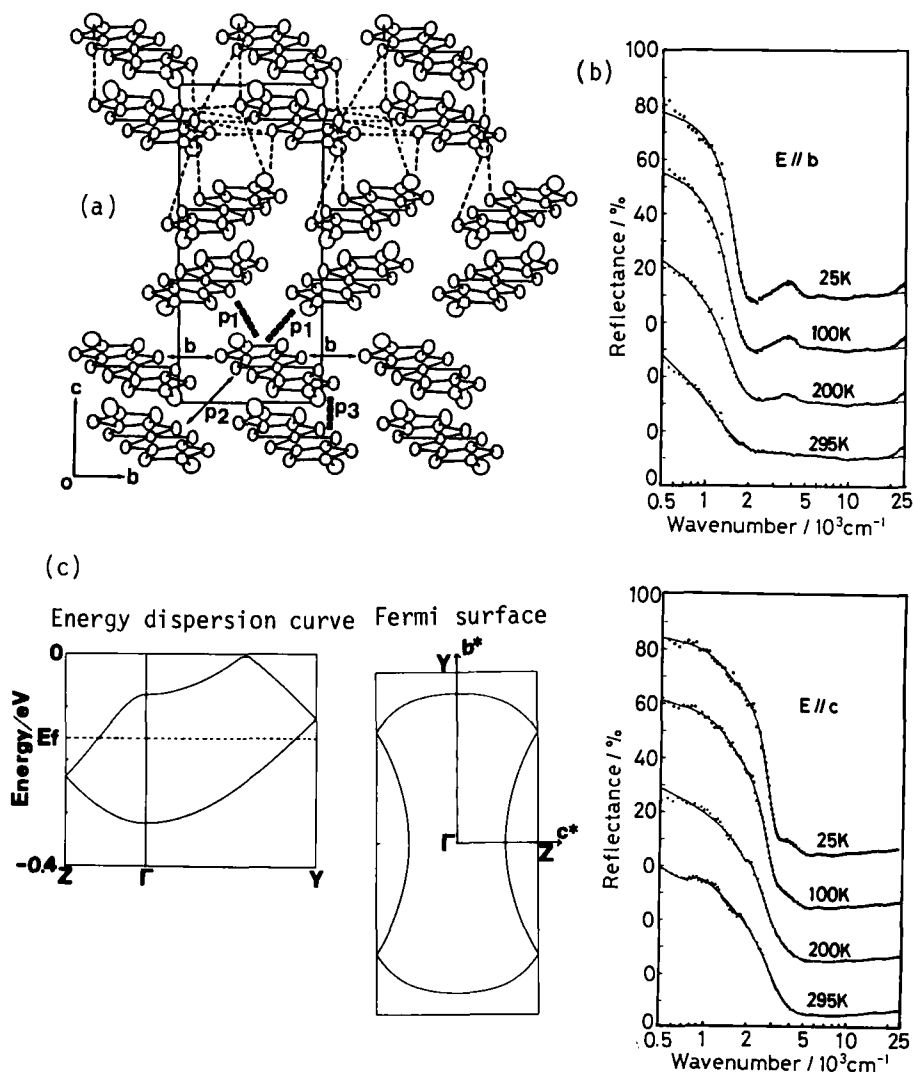


FIGURE 4 (a) Crystal structure, (b) reflectance spectra, and (c) calculated band structure of $\text{Et}_2\text{Me}_2\text{N}[\text{Ni}(\text{dmit})_2]_2$.

lowest and second lowest band calculated from these parameters. The shapes of both energy dispersion curve and Fermi surface roughly agree with those calculated by Extended Huckel method.

α -EDT-TTF[Ni(dmit)₂]

This salt is metallic down to 4.2K.⁹ Figure 5 shows the reflectance spectra and crystal structure of this salt. In this salt there are two different kinds of conduction sheets. One is made of [Ni(dmit)₂] units, and the other is made of EDT-TTF units. Both conduction sheets have column structure and each column is elongated along either b-axis (for the [Ni(dmit)₂]'s sheet) or [110] axis (for the EDT-TTF's sheet). The reflectance spectra are well reproduced by the Drude formula for both polarizations. The plasma frequencies obtained by use of the Drude model (Eq.(1)) are $8.6 \times 10^3 \text{ cm}^{-1} (//b)$ and $5.6 \times 10^3 \text{ cm}^{-1} ((001) \perp b)$. The ratio of oscillator strength is 2.4, suggesting small anisotropy within the ab-plane.

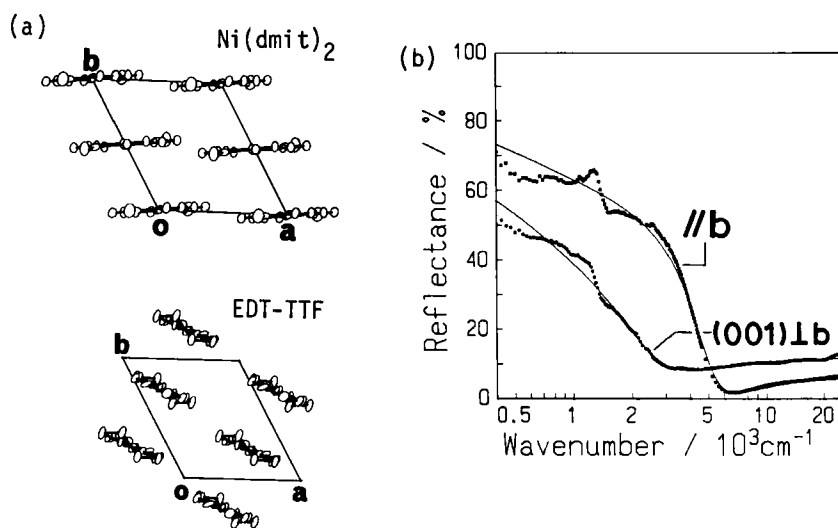


FIGURE 5 (a)Crystal structure and (b)reflectance spectra of α -EDT-TTF[Ni(dmit)₂].

Discussion

As shown in Fig. 1 ~ Fig. 5, strong and broad dispersion about $10 \sim 11 \times 10^3 \text{ cm}^{-1}$ appears in the [Pd(dmit)₂] salts, but not in any of [Ni(dmit)₂] salts. This dispersion is assigned to the one originated

from the intermolecular interaction. The intensity parameter, I_{σ} , of this broad band was estimated from the observed conductivity spectrum by the following equation,

$$I_{\sigma} = 8 \int_{5000\text{cm}^{-1}}^{15000\text{cm}^{-1}} \sigma(\omega) d\omega \quad (5)$$

The values of intensity parameters, obtained from the conductivity spectra at various temperatures, are [$200 \times 10^6 \text{cm}^{-2} \sim 240 \times 10^6 \text{cm}^{-2}$] for $\text{Cs}[\text{Pd}(\text{dmit})_2]_2$, and [$160 \times 10^6 \text{cm}^{-2} \sim 190 \times 10^6 \text{cm}^{-2}$] for $\text{Me}_4\text{As}[\text{Pd}(\text{dmit})_2]_2$. Such a large intensity is quite anomalous for the CT transition in 2:1 salts. In order to understand this phenomenon, let us consider the three cases (1)-(3) shown in Fig. 6. For simplicity, we will assume that the value of t is the same for HOMO's, and for LUMO's within the dimer and that neglect all of other transfer integrals. This assumption is consistent with the results of the calculation of the overlap integral.

In the material with strong dimerization, the inter-band transition, having the character of the transition from dimer's bonding orbital to its antibonding orbital, appears at the energy of $2t$ in the case (1). (See Fig. 6(a).) The intensity parameter is expressed by $I_{\sigma} = 4\pi e^2 d^2 t / V \hbar^2$ in this case, where V and d are the volume of the dimer, and a -axis component of the spacing of the dimer. If we assume $t = 0.7 \text{eV}$, the optical transition is expected to appear at the excitation energy of $2t = 1.4 \text{eV}$ ($11 \times 10^3 \text{cm}^{-1}$) with the intensity parameter $72 \times 10^6 \text{cm}^{-2}$ for the //a spectrum. This intensity value is too small to explain the observed one.

If the energy difference between HOMO and LUMO is larger than $2t$ as in the case (2), the intensity parameter should be the same as in the case (1). (See Fig. 6b.) Hence the case (2) also fails to explain the observed large intensity parameter.

If the energy difference between HOMO and LUMO is smaller than $2t$ as shown in the case (3), we can expect a large intensity parameter, because two electrons filling the LUMO band, as well as one hole in the HOMO band in the dimer are expected to give transitions corresponding to the $10 \sim 11 \times 10^3 \text{cm}^{-1}$ dispersion. (See Fig. 6c.) Therefore the intensity parameter could be three times as much as the value estimated for the cases (1) and (2), which is consistent with

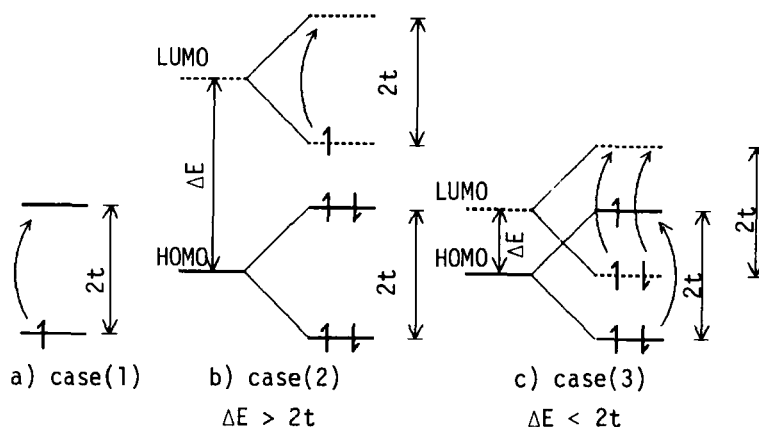


FIGURE 6 Schematic energy level of $\text{Cs}[(\text{Pd}(\text{dmit})_2)_2]$, and $\text{Me}_4\text{As}[(\text{Pd}(\text{dmit})_2)_2]$

the observation. Thus we can conclude that the conduction band of this salt is mainly made from HOMO. This conclusion seems to be consistent with the isotropic plasma frequencies in the $[\text{Pd}(\text{dmit})_2]$ salt.

This work was supported by the Grant-in-Aid for Encouragement of Young Scientist(No. 01740259) and Scientific Research (No. 01470004) from the Ministry of Education, Science and Culture.

REFERENCES

1. L. Brossard, M. Ribault, M. Bousseau, L. Valade, and P. Cassoux, *C. R. A. S.*, **302**, 205(1986).
2. A. Kobayashi, H. Kim, Y. Sasaki, S. Moriyama, Y. Nishio, K. Kajita, W. Sasaki, R. Kato, H. Kobayashi, *Synthetic Metals*, **27**, B339(1988).
3. L. Brossard, H. Hurdequint, M. Ribault, L. Valade, J. P. Legros, P. Cassoux, *Synthetic Metals*, **27**, B157(1988).
4. H. Kim, A. Kobayashi, Y. Sasaki, R. Kato, and H. Kobayashi, *Chem. Lett.*, **1987**, 1799.
5. We made the resistivity measurements for two samples prior to the optical measurements in this material. They showed different behavior in the resistivity measurements, but their reflectance spectra were almost same all over the temperature region measured.
6. R. A. Clark, A. E. Underhill, *Synthetic Metals*, **27**, B515(1988).
7. A. Kobayashi, H. Kim, Y. Sasaki, K. Murata, R. Kato, H. Kobayashi, *J. Chem. Soc.*, in press.
8. R. Kato, H. Kobayashi, H. Kim, A. Kobayashi, Y. Sasaki, T. Mori, H. Inokuchi, *Chem. Lett.*, **1988**, 865.
9. R. Kato, H. Kobayashi, A. Kobayashi, T. Naito, M. Tamura, H. Tajima, H. Kuroda, *Chem. Lett.*, **1989**, 1839.